An Analysis of Recovery Motion of a Man Wearing Physical Assistant Robot in Response to Collision

Yasuhiro Akiyama*, Ryota Kushida*, Yoji Yamada*and Shogo Okamoto*
*Department of Mechanical Science and Engineering
Graduate School of Engineering, Nagoya University, Nagoya, Japan

***Abstract*—Physical assistant robots are expected to be able to assist in our working and daily lives. However, safety problems arise when robots are used in indoor environments with obstacles. The focus of this study was on collision of the side of a robot with an obstacle, and the recovery motion after the collision was measured. A healthy young man participated in this experiment. Two different types of recovery motions were observed. These two motions differed in the degree of deceleration of the body rotation in the horizontal plane. The part of the robot and the timing of the collision with the obstacle affected the recovery motion strategy. A collision at the hip side in the middle swing phase might be the most severe condition from which to recover, among those considered in this study. The results of this study will be helpful in improving the safety of the use of physical assistant robots.**

***Index Terms*—Physical assistant robot, Safety, Recovery motion**

I. Introduction

In many countries, population aging has been causing problems such as increasing demands for nursing care and decreasing numbers of workers. Physical assistant robots, which are attached to a human body and apply torque through cuffs and shoes, are thought to be effective solutions to such social problems because they can assist in the activities of daily living and rehabilitation of the wearer [1], [2]. Furthermore, physical assistant robots increase labor productivity by decreasing workloads [3].

However, the use of physical assistant robots requires greater attention to safety than the use of industrial robots because of the close contact into which such robots come with users. Among the anticipated hazards, a fall is a serious hazard especially for the elderly [4]. However, the effect of a physical assistant robot on the risk of a fall has rarely been analyzed, except in a few studies [5]. Thus, ISO13482 [6], which is the industrial standard that addresses the safety of physical assistant robots, only addresses contact safety.

For a normal gait without physical assistant robot, falling as a result of tripping has been analyzed previously in many ways [7], [8], and the associated recovery motions have been categorized [9]. This knowledge is helpful in evaluating the risk of a fall induced by wearing a physical assistant robot. Furthermore, the environments in which physical assistant robots are being used are becoming more complex as they are increasingly coming to be used in daily living. For example, doors are typical features of an indoor environment that the user of a physical assistant robot encounters in a building or house. A collision between a robot and the casing of a door was taken as the focus of this study because it is difficult to avoid such a collision in indoor environment.

Fig. 1. MALO

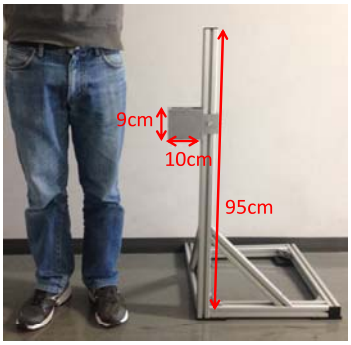

Fig. 2. Obstacle

The main objective in this study was measurement of the recovery motion of the user of the robot for the purpose of identifying the best recovery strategy and the factors that determine which recovery motion should be made. Improving the understanding of the recovery strategy that a robot should apply in response to a collision will help in designing physical assistant robots to avoid and mitigate falls.

II. Method

A. Apparatus

1) Physical assistant robot: The Motor-Actuated Lower-limb Orthosis (MALO), developed in our lab, was used in this study. MALO, which consists of a hip orthosis and a knee-ankle-foot orthosis, is shown in Fig. 1. MALO has one degree of freedom in the sagittal plane at the hip, knee, and ankle joint of each leg. The hip and knee joints of each leg are actuated by DC motors (RE40, Maxon Motor, Switzerland) and the other joints move freely. MALO is attached to a wearer using a corset, cuffs, and shoes. In this study, aluminum plates were attached to the sides of the thigh links of the leg to serve as surfaces that would come into contact with the obstacle.

The pattern of the assist torque generated by MALO was synchronized with the user's gait cycle [5]. In this study, the gait cycle was defined as the time elapsed between consecutive heel strikes of one leg, which is a typical definition. Torque was applied to the hip joint during 5% to 20% of the gait cycle to the extension direction and 55% to 70% to the flexion direction. Then, the knee joint was supported to the extension direction during 80% to 90% and flexion direction during 40%

to 55%. The algorithm that synchronizes the robot's motion to the user's gait cycle is a popular motion assistance method for physical assistant robots [10], [11]. The algorithm assists in the forward motion of the body mass during the stance phase and assists to swing leg. The applied torque was 10 N·m for the hip joints and 6.5 N·m for the knee joints. These torque levels are approximately 25% of the average torque for human gait motion. In addition, MALO compensates for its kinetic friction.

2) Experimental devices: A 7-meter straight walking lane was used in this study. The first 3 m and the last 1 m of the lane were the acceleration and deceleration areas. The motion of the subject in the middle area was recorded by a motion capture system (MAC 3D System, Motion Analysis Corporation, CA) and video camera (SONY, Japan). In addition, mobile six-axis force plates (M3D, Tech Gihan Co., Ltd., Japan) were attached to each sole to measure the ground reaction force.

An obstacle, shown in Fig. 2, was used to cause collisions with the subject. The height of the obstacle was adjustable up to 1 m. A six-axis force sensor (DynPick, WACOH, Japan) was attached to the contact surface. The obstacle was randomly placed on the lateral side of the lane to strike the side of the MALO. The subject wore goggles with the lower parts of the lenses covered to prevent anticipation and preparation.

For safety, the subject was connected to a gondola on the ceiling using a safety harness to prevent him from falling. Thus, the subject was supported by the harness when his torso lowered to some degree. However, the harness did not disturb the normal gait motion of the subject because of the allowance provided. The subject also wore knee protectors and ankle supporters.

B. Protocol

The experiment was performed with the permission of the institutional review board of Nagoya University. The subject was a healthy twenty-three-year-old male whose height was 170.6 cm and whose weight was 62.0 kg. He was instructed to walk at a constant speed and stride length along the walking lane, to which the obstacle had been attached in advance. Contact between the side of the physical assistant robot and the obstacle occurred occasionally. Overview of these experimental devices were shown in Fig. 3.

Collisions occurred during the initial swing phase, defined as 60% to 75% of the gait cycle, or during the middle swing phase, defined as 75% to 85% of the gait cycle. The collision timing was controlled by changing the position of the obstacle. The obstacle collided with the upper thigh or lower part of the thigh of the MALO, depending on the height of the obstacle (approximately 55 or 80 cm). These collisions were produced on both the left and right sides of the subject to prevent asymmetric preliminary avoidance motion of the subject. Combining these parameters, contact occurred at the hip side or knee side of the thigh during the initial swing phase or at the hip side during the middle swing phase. These conditions were selected on the basis of preliminary experiments because of the seriousness of their effects on gait motion. In addition,

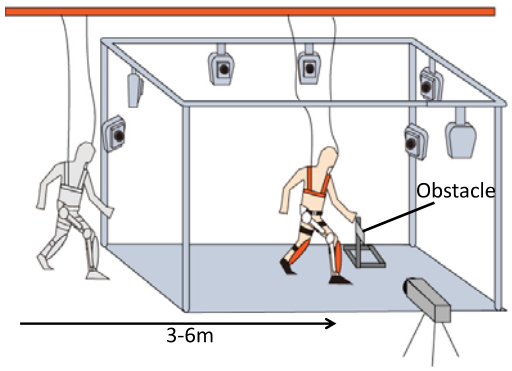

Fig. 3. Experimental overview

TABLE I
TIMING OF THE COLLISION AMONG GAIT CYCLE

	Hip initial	Hip middle	Knee initial
Right side collision [%]	74.9	84.8	67.9
Left side collision [%]	69.9	77.8	71.9

the order of the conditions was randomized between trials. In total, six collision trials (two trials of each condition) and six dummy trials, where no obstacles were used, were successfully recorded.

C. Data processing

The positions of the markers attached to the body of the subject, were recorded at a frequency of 100 Hz and filtered at 6 Hz using a Butterworth filter. The marker positions were used to calculate the attitude and position of the pelvis, torso, and footmarks. The timing of the heel contact was detected when the ground reaction force exceeded 10 N. The timing of the collision was defined as being when the force sensor of the obstacle detected the contact. The data from the force sensor, which performed at 1 kHz, of the obstacle was also used to calculate the force impulse and peak force of the collision.

III. RESULTS

The gait timings of the dummy cases were validated first. The subject walked at a speed of 4.6 km/h on average, with a standard deviation of 0.4 km/h. Each stride consisted of a 0.70 ($\pm$ 0.05) m step length and a 1.08 ($\pm$ 0.03) s stride time. These values suggest that the subject's gait was normal for a typical young person. The collision timing of each trial is listed in Table I. The initial swing phase started at 60% and ended at 75%. The middle swing phase started at 75% and ended at 85%. Thus, the collision timings successfully included within the conditions considered.

Position of footprints are shown in Figs. 4 and 5. In these graphs, footprint was defined as the line between the position of toe marker and heel marker when the foot contacted to the ground totally. Numbers of the steps were placed on the toe side. The number of footprint started from the step just before the collision in Fig. 4. Then, following two steps could

a black dot stands for the position of the obstacle

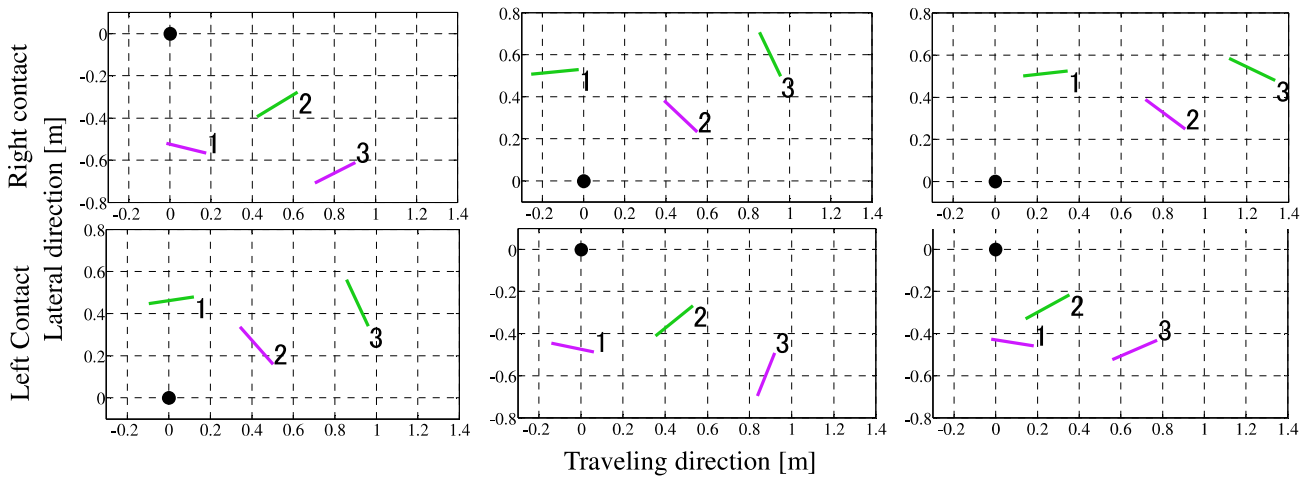

Fig. 4. Footprint of collision cases (left: collision with the hip during the initial swing phase, middle: collision with the hip during the middle swing phase, right: collision with the knee during the initial swing phase)

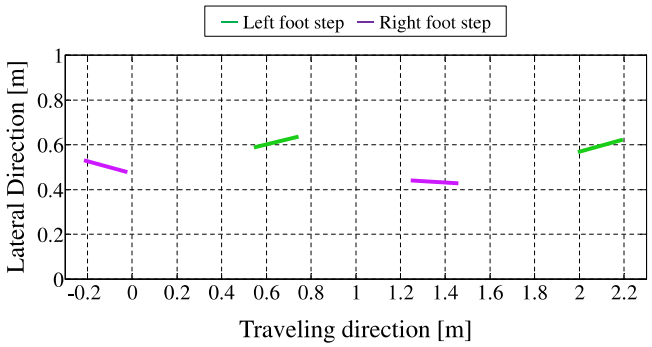

Fig. 5. Representative footprint of normal gait motion

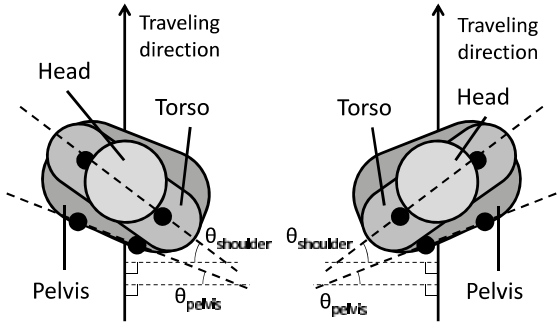

Fig. 6. Definition of rotation angles of shoulder and pelvis (left: right side collision, right: left side collision)

be shown in the figure. At the same time, the position of the obstacle was plotted by a black dot.

A representative pattern from the dummy trials is shown in Fig. 5. As Fig. 5 shows, the step length during normal walking was approximately 0.7 m, which corresponded to the average step length mentioned before.

However, footprints of collision cases differed from that of normal cases as shown in Fig. 4. The step length just after tripping (step no. 2) became smaller than that for a normal step. In addition, the direction of the foot differed from that during normal walking, especially during the second step (step no. 3): the subject opened his leg in the coronal plane. Thus, the subject immediately lowered the swing leg when the collision occurred. He then spread the opposite leg. The same tendencies were observed in every trial in response to a collision.

It is important to consider the rotation of the body in analyzing the recovery motion of the subject. Geometry of rotation angles are shown in Fig. 6. The direction of the shoulder was defined using line that connected the markers of left and right shoulders. Then, the angle of the torso in the horizontal plane was defined as the lines between the direction of shoulder and transverse direction. The angle of the pelvis was defined as the same manner as the torso using markers of the posterior superior iliac spine. The rotation angles of the pelvis and torso in the horizontal plane at the time of contact and during the succeeding two steps are compared in Fig. 7. The rotation angle becomes zero when the body is along with the walking lane. To analyze the trials with collisions on different sides at the same time, rotations toward the side at which obstacle was placed were assigned positive values. The results suggest that the difference in the motions of the tripping legs was not apparent.

According to Fig. 7, the rotation angle differed drastically depending on the collision timing and part. The recovery motion differed between trials, with continuous or decelerated rotation occurring after the first step in hip initial collision cases. However, both the shoulder and pelvis rotated continuously in all hip middle collision cases. In contrast, the increases in these angles decelerated after the first step in all of the knee initial collision cases. In all of the trials, although

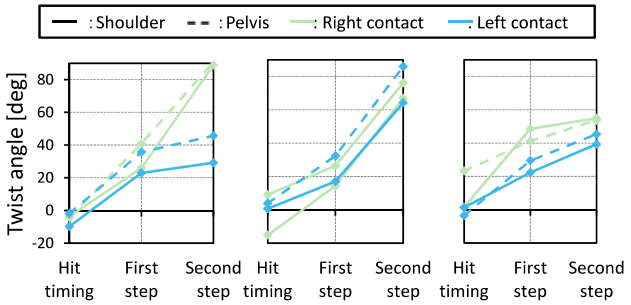

Fig. 7. Shoulder and pelvis rotational angle (left: collision with the hip during the initial swing phase, middle: collision with the hip during the middle swing phase, right: collision with the knee during the middle swing phase)

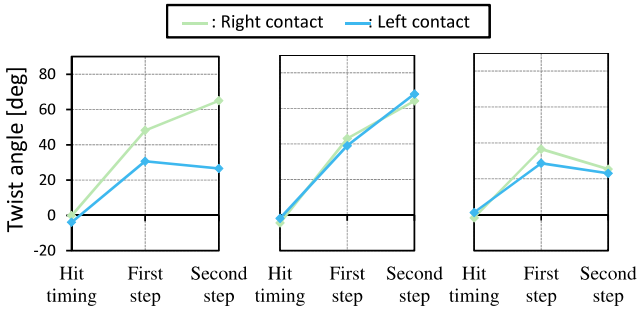

Fig. 8. Foot rotational angle (left: collision with the hip during the initial swing phase, middle: collision with the hip during the middle swing phase, right: collision with the knee during the middle swing phase)

there were some differences between the pelvis and shoulder angles, the largest difference between pelvis rotation angle and shoulder rotation angle, which meant the twist of upper body, was approximately 30 deg.

The angle of the foot in the horizontal plane, shown in Fig. 8, was the same as the angle of the footprint shown in Fig. 4. Rotations from the traveling direction toward the side on which the obstacle was placed were assigned positive values, as with the body rotation angles.

Although the angle of the foot increased just after contact in all cases, it decreased during the second step in some cases. In addition, the increase in the rotation angle decelerated even in the other cases. These trends depended on the condition of the contact timing and the contact part. The former pattern was mainly observed in the knee initial collision cases, whereas the latter pattern was mainly observed in the hip middle cases. Both patterns were observed in the hip initial cases. These characteristics corresponded to the rotation of the body shown in Fig. 7.

The peak force acting on the obstacle in the traveling direction and the impulse are shown in Fig. 9. These graphs suggest that the peak force in the knee initial cases were approximately double those in the hip cases. However, the magnitudes of the impulses did not differ drastically.

IV. Discussion

As is the common tendency, the subject rotated his whole body toward the side on which the obstacle was placed during

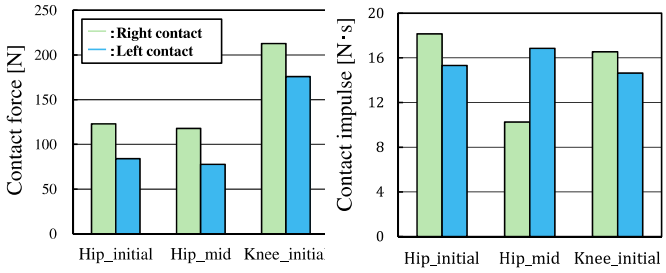

Fig. 9. Force and impulse at contact (left: peak contact force, right: impulse of contact force)

the recovery motion. However, the recovery motions of the trials could be categorized as following one of two strategies, deep rotation or short rotation. Sometimes, the subject continued to rotate his body and foot even during the second step. This deep rotation could be observed in the hip middle collision case and some of the hip initial cases. In contrast, a short rotation accompanied a rapid decrease in foot rotation. This motion was observed in the knee initial contact cases and some of the hip initial cases.

The most significant difference between these two strategies appeared during the second step. In the case of short rotation, the foot angles decreased at the second step and the body rotation slowed down, which suggests that the subject tried to recover the direction of his body. In contrast, although the same tendency (the foot angle becoming smaller than the body angle) was observed during the second step in the deep rotation cases, the foot angle did not decrease. However, even in the deep rotation cases, deceleration of the foot rotation could be a sign of deceleration or stopping of body rotation. For both strategies, even during rotation of the body, the difference between the pelvis rotation angle and the shoulder rotation angle remained approximately 30 deg, as mentioned previously. This limitation of the torso twist angle was probably due to how MALO is attached to the torso. Because MALO is attached to the torso of the subject using a corset for effective torque translation, it limits twisting of the torso to some degree. Thus, the rigidity of the corset probably affected the shoulder rotation.

Although the number of trials was not sufficient to evaluate the recovery strategy statistically, the results suggest that the selection or development of the recovery motion clearly depended on the timing and body part of the contact. In the hip middle collision case, the deep rotation recovery was observed, whereas the short rotation recovery was observed in the knee initial collision case. In addition, both patterns appeared in the hip initial collision case. From the perspective of kinetics, the contact position affected the distribution of the reaction force and moment. When the obstacle struck the lateral part of the robot, the swing leg was pushed back and the body rotated in the horizontal plane. The rotation moment might have become larger when the hip side collided with the obstacle because the hip side is closer to the pelvis, so the contact force affected the body directly. On the other hand, a contact force at the knee side was probably transformed into an extension moment of

the hip joint in the sagittal plane. Thus, it was probably more difficult to stop the rotation of the body in the horizontal plane in the hip contact case. The timing of the contact also affected the ability of the subject to stop his body from rotating. During the initial phase of the swing motion, the center of mass of the subject remained close to the stance leg. However, it gradually moved forward and increased in speed when the swing motion entered the middle phase. Thus, the contact in the initial phase might be easily compensated for by strengthening the muscle force of the stance leg. As a result, a collision at the hip side in the middle swing phase might be the most severe condition from which to recover, among those considered in this study. In contrast, it is probably relatively easy to overcome a collision at the knee side in the initial swing phase. The hip initial case lies between these two other cases.

Because of the marginal numbers of trials, there was no time for the subject to get accustomed to the disturbance during this experiment. However, increased number of trials are required to obtain general trend. Thus, randomization of the disturbed conditions becomes more important to prevent the learning of the subject. However, even using such countermeasures, it probably will be not easy to increase the number of trials for each subject. This limitation becomes a problem when inspecting the effect of various assist algorithm to the recovery motion. Limited number of trials increases the importance of the simulation. The fundamental strategy of the recovery motion obtained by the experiment will help to assume the recovery strategy of the wearer.

V. Conclusions

The goal of this study was to detect the strategy used by a human wearing a physical assistant robot to recover from a collision with an obstacle. In the experiments conducted, the obstacle struck the side of the robot, an occurrence that was assumed to be similar to the wearer failing to pass through a doorway.

In all cases, the subject rotated his body toward the side on which the obstacle was placed after contact with the obstacle. However, the subject's motions in the trials differed considerably and could be separated into two patterns: deep rotation and short rotation. Deep rotation occurred when the obstacle hit the upper thigh part of the wearer in the middle swing phase. In such cases, the rotation of the body did not stop even at the second step after the collision occurred. In contrast, short rotation occurred when the obstacle hit the lower part of the thigh of the wearer in the initial swing phase. The subject successfully stopped the rotation of his body and decreased the rotation angle. In addition, an analysis from a kinetic perspective suggests that the moment in the horizontal plane differed depending on the part of the robot struck and the motion phase in which the collision occurred. The experimental results are consistent with the kinetic analysis and suggest that the factors that determine the recovery motion taken were successfully detected.

Acknowledgment

This work was supported by JSPS KAKENHI Grant Number 26750121.

References

[1] K. Yasuhara, K. Shimada, T. Koyama, T. Ido, K. Kikuchi, and Y. Endo, "Walking assist devices with stride management system," *Honda R&D Technical Review*, vol. 21, no. 2, pp. 54–62, 2009.

[2] K. Suzuki, G. Mito, H. Kawamoto, Y. Hasegawa, and Y. Sankai, "Intention-based walking support for paraplegia patients with robot suit hal," *Advanced Robotics*, vol. 21, pp. 1441–1469, 2007.

[3] H. Kobayashi, T. Aida, and T. Hashimoto, "Muscle suit development and factory application," *International Journal of Automation Technology*, vol. 3, no. 6, pp. 709–715, 2009.

[4] J. S. Brach, S. Perera, S. Studenski, M. Katz, C. Hall, and J. Verghese, "Meaningful change in measures of gait variability in older adults," *Gait & Posture*, vol. 31, pp. 175–179, 2010.

[5] Y. Akiyama, I. Higo, Y. Yamada, and S. Okamoto, "An analysis of recovering motion of human to prevent fall in responce to abnormality with a physical assistant robot," in *IEEE International Conference on Robotics and Biomimetics*, 2014, pp. 1493–1498.

[6] ISO, "Robots and robotic devices – safety requirements for personal care robots," International Organization for Standardization, Tech. Rep. ISO 13482:2014, 2014.

[7] T.-Y. Wang, T. Bhatt, F. Yang, and Y.-C. Pai, "Adaptive control reduces trip-induced forward gait instability among young adults," *Journal of Biomechanics*, vol. 45, pp. 1169–1175, 2012.

[8] M. Pijnappels, M. F. Bobbert, and J. H. van Dieën, "Changes in walking pattern caused by the possibility of a tripping reaction," *Gait and Posture*, vol. 14, pp. 11–18, 2001.

[9] J. J. Eng, D. A. Winter, and A. E. Patla, "Strategies for recovery from a trip in early and late swing during human walking," *Experimental Brain Research*, vol. 102, no. 2, pp. 339–349, 1994.

[10] G. Taga, Y. Yamaguehi, and H. Shimizu, "Self-organized control of bipedal locomotion by neural oscillators in unpredictable environment," *Biological Cybernetics*, no. 65, pp. 147–159, 1991.

[11] L. Wang, S. Wang, E. H. F. van Asseldonk, and H. van der Kooij, "Actively controlled lateral gait assistance in a lower limb exoskeleton," in *IEEE/RSJ International Conference on Intelligent Robots and Systems*, 2013, pp. 965–970.